Communication

Interfacial Polymerization within a Simplified Microfluidic Device: Capturing Capsules

Elizabeth Quevedo, Jeremy Steinbacher, and D. Tyler McQuade

J. Am. Chem. Soc., **2005**, 127 (30), 10498-10499• DOI: 10.1021/ja0529945 • Publication Date (Web): 09 July 2005

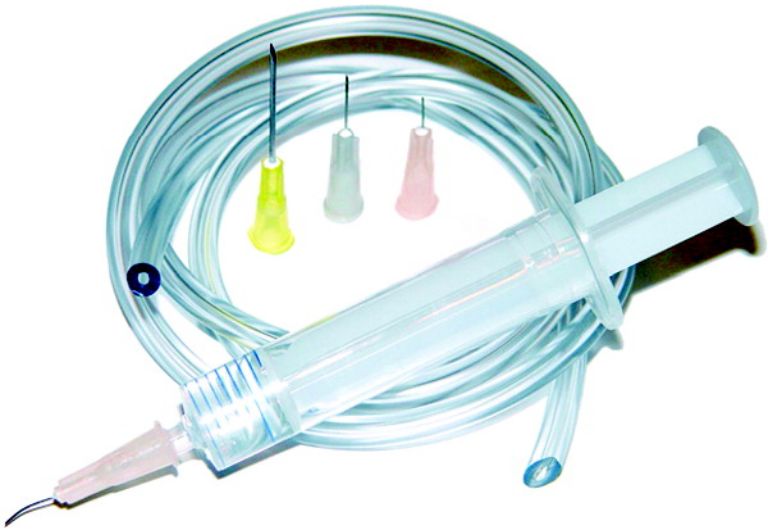

J|A|C|S
COMMUNICATIONS

Published on Web 07/09/2005

Interfacial Polymerization within a Simplified Microfluidic Device: Capturing Capsules

Elizabeth Quevedo, Jeremy Steinbacher, and D. Tyler McQuade*

Cornell University, Department of Chemistry and Chemical Biology, Baker Laboratory, Ithaca, New York 14853-1301

Received May 7, 2005; E-mail: dtm25@cornell.edu

Unique fluid fields generated in microfluidic devices can control self-assembly,[1] crystallization,[2,3] and reagent mixing.[4] Quake et al.,[5] Weitz et al.,[6] and Nisisako et al.[7] showed for example that emulsion droplets can be formed and organized into a wide range of patterns within microfluidic channels. Emulsions are created by colliding two immiscible liquids, water and oil, to form either an oil-in-water or a water-in-oil emulsion at the junction where the two liquids meet. To date, such emulsions have been captured by coascervation,[8] by photoinitiated polymerization to create solid beads,[9] by a double emulsion method to create hollow capsules,[10] or by interfacial polymerization.[11]All three methods use a two-step procedure where the droplet is first produced at a fluid junction and then polymerized downstream. In the case of the capsules, Whitesides et al. used axisymmetic flow-focusing to form droplets containing one monomer that are then carried via a hexadecane solution to a second monomer downstream from droplet formation. The technique, though elegant and widely employed,[10,13] is much more complicated than necessary.

An alternate approach to forming capsules within a microfluidic device relies on interfacial polymerization as the droplet is formed. By adding monomers and cross-linkers to each phase, the emulsions can be captured as microcapsules without the use of carrier fluids that otherwise complicate the system. The overall result is semipermeable, micrometer-sized capsules that can be collected. Herein, we describe the use of interfacial polymerization to create fluid-filled spheres that are captured as they are formed. The key to our success is the use of a new simple microfluidic device where capsules are snapped off as they are formed. This new approach not only yields capsules but also illustrates a much simpler approach to microfluidics.

Ideally, fluidic devices should allow for rapid and cost-effective prototyping. Materials currently employed to create microfluidic devices include elastomers, glass, and silicon. Two materials most popularly used to make microfluidic devices compatible for organic reactions are "liquid Teflon"[14] and those made from silicon/glass.[15] These approaches, however, require expensive monomer synthesis or specialized techniques, and the resulting microfluidic devices are easily clogged with polymer debris.[11] To overcome these drawbacks, we report a microfluidic system using common laboratory tubing and needles. As illustrated in Scheme 1, immiscible solutions are introduced into the device by two separate syringe pumps, allowing independent flow rate variation. For this initial report, the aqueous phase is contained within a 50-mL syringe and flows through poly(vinyl chloride) (PVC) tubing ($^1/_{16}$ in. i.d. × $^3/_{16}$ in. o.d.); the organic solution is dispensed from a 1-mL or 5-mL syringe and introduced via a 30-gauge needle inserted through the wall of the PVC tubing and situated in the middle of the channel (Figure 1).

Regardless of its simplification, this tube and needle design yields fluidic behavior similar to traditional microfluidic devices. Flow

Figure 1. Photograph of fluidic device including needle and dye-filled organic droplets dispersed in the continuous aqueous phase.

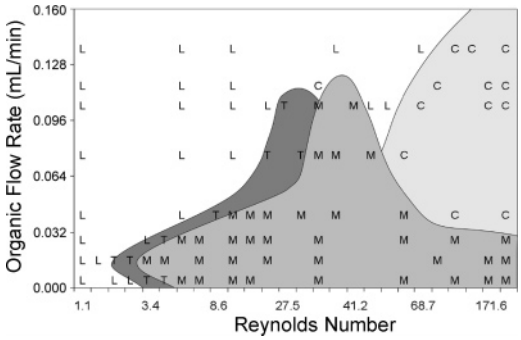

Figure 2. Phase diagram depicting the flow regimes as functions of Reynolds and organic flow rate. Each letter is a data point representing laminar flow (L), monodisperse droplets (M), transition between laminar flow and monodisperse droplets (T), and chaotic flow (C).

Scheme 1. Schematic of Fluidic Device

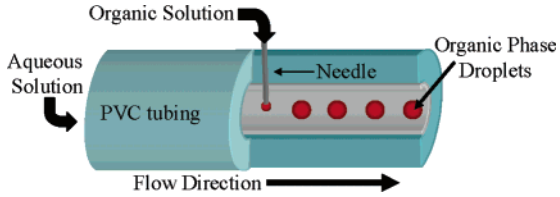

behavior was measured as a function of organic and aqueous flow rates using glycerol (30% w/v) in deionized water as the continuous phase and a 3:1 cyclohexane/chloroform mixture with 2% (v/v) Tween 80 as the dispersed phase. Figure 2 is the phase diagram illustrating the regions favorable for laminar flow (L), the transition between laminar flow and monodisperse droplets (T), monodisperse droplets (M), and chaotic flow (C). Each letter in Figure 2 represents a data point collected. These results are consistent with those observed by Nisisako[9] in a microfluidic device and illustrate that this simple tubular design exhibits phase behavior similar to that of standard microfluidic devices with rectangular channels.

On the basis of this initial success, we examined the interfacial polymerization of the monodisperse flow phase to generate a polyamide shell.[16] We expected that our tubing/needle design would facilitate interfacial polymerization relative to classic microfluidic devices because the disperse phase is entirely surrounded by the continuous phase, as seen in Scheme 1. Only axisymmetric devices can achieve this coaxial geometry, and these devices are much more

10.1021/ja0529945 CCC: $30.25

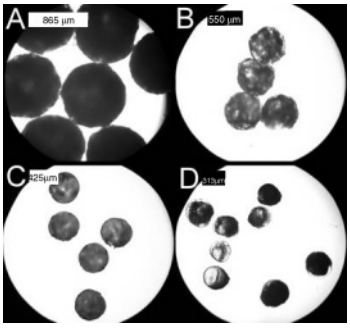

Figure 3. Light microscope images of capsules in water formed with constant organic flow rate (0.141 mL min^{-1}) and increasing aqueous flow rate: (A) 2.00 mL min^{-1}; (B) 11.0 mL min^{-1}; (C) 13 mL min^{-1}; (D) 25 mL min^{-1}. See Supporting Information for a general synthetic route. Field of view is constant; magnification is 10×.

Table 1. Mean Capsule[a] Size as a Function of Aqueous Flow Rate and Corresponding Coefficients of Variation (CV)

aqueous flow (mL/min)	mean capsule size (μm)	CV (%)[b]
2.0	865	3.5
5.0	704	4.6
7.5	554	5.7
11	550	4.9
13	425	3.3
18	365	8.6
25	313	8.2

[a] See Supporting Information for a general synthetic route. [b] One hundred capsules formed at each flow rate were measured via the ocular scale bar on the light microscope to determine mean capsule dimaters and corresponding coefficients of variation.

complicated. Another advantage of our tubular device over a traditional microfluidic system is that, should the device become clogged, we simply replace the tubing, yielding a clean and functional apparatus within seconds. To capture capsules, we used polyethyleneimine (PEI) in the continuous phase (aqueous) and a mixture of sebacoyl and trimesoyl chloride for the dispersed phase (organic). Contact between the two solutions at the needle/tube junction resulted in oil filled, polyamide capsules.

The effect of aqueous flow rate on capsule size was explored by holding the organic disperse flow rate constant and by varying the aqueous flow rate. It was found that capsule size gradually decreased with increased aqueous flow rate and, hence, with increasing Reynolds number (Figure 3). Table 1 depicts the array of capsule sizes created over a range of continuous phase flow rates. Over the entire 550-μm range, the capsule diameters maintained a CV of less than 9%. Moreover, we predict that by using a needle with a smaller aperture monodispersed capsules with smaller diameters may form. Alternatively, the disperse phase flow rate could be slowed to decrease the capsule size. Furthermore, we noted that the diameter CV of the unpolymerized emulsions is smaller than the diameter CV of the capsules. We suggest that the higher CV is due to deformation of the shell as capsules exit the device.

Once the emulsion interfaces were polymerized to form capsules, they were characterized by scanning electron microscopy (SEM) to determine shell characteristics such as the surface topology and thickness. The SEM images in Figure 4A are representative of the entire population in this system and show well-defined capsules with robust shells (Figure 4). The initially plastic capsules mature into hard spheres that have fibrous shells as observed in the SEM images of partially crushed capsules (Figure 4B).

In conclusion, we have demonstrated that simple flexible tubing and narrow gauge needles can replace classic elastomeric and hard

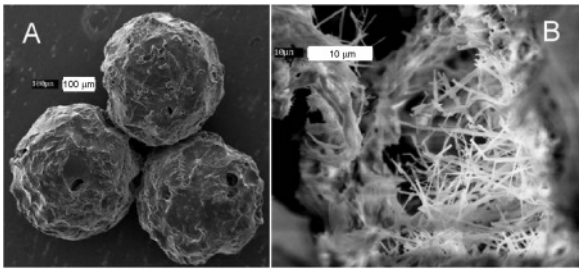

Figure 4. (A) SEM images of microcapsules prepared under the following conditions: aqueous flow rate = 13.0 mL min^{-1}, organic flow rate = 0.141 mL min^{-1}. Magnification is 133×, scale bar is 100 μm. (B) High magnification image of the interior of capsule wall after intentional rupture via mechanical pressure. Magnification is 4.99 k×, scale bar is 10 μm.

material microfluidic devices. We feel that this tubing approach can be interfaced with the same valves and spectrophotometers as those for HPLCs and that tubing of very narrow diameter can be purchased to allow further scale down. The new design yields laminar, transitional, droplet, and chaotic phases in the same way as classic devices. An added advantage of the reported system is that both the tubing and needle are tubular and we can, therefore, introduce a disperse phase into the center of a continuous phase. This coaxial feature allows interfacial polymerization to occur without interference from the walls. We demonstrated that capsules with low CVs and a range of sizes are captured using interfacial polymerization. The capsule shells exhibit a unique fibrous structure that may be a ramification of polymerization within the fluid fields of the device. We are currently examining the scope of shapes that can be captured and the range of interfacial chemistry that can be used.

Acknowledgment. We thank the Beckman Foundation, Cornell University, the Dreyfus Foundation, ARO DAAD19-02-1-0275 Macromolecular Architecture for Performance (MAP) MURI, NSF (SENSORS), and the Cornell Center for Materials Research.

Supporting Information Available: Device design, experimental procedures, and further capsule images and characterization. This material is available free of charge via the Internet at http://pubs.acs.org.

References

(1) Kenis, P. J. A.; Ismagilov, R. F.; Whitesides, G. M. *Science* **1999**, *285*, 83−85.
(2) Zheng, B.; Tice, J. D.; Ismagilov, R. F. *Adv. Mater.* **2004**, *16*, 1365−1368.
(3) Zheng, B.; Tice, J. D.; Roach, L. S.; Ismagilov, R. F. *Angew. Chem., Int. Ed.* **2004**, *43*, 2508−2511.
(4) Zheng, B.; Tice, J. D.; Ismagilov, R. F. *Anal. Chem.* **2004**, *76*, 4977−4982.
(5) Thorsen, T.; Roberts, R. W.; Arnold, F. H.; Quake, S. R. *Phys. Rev. Lett.* **2001**, *86*, 4163−4166.
(6) Link, D. R.; Anna, S. L.; Weitz, D. A.; Stone, H. A. *Phys. Rev. Lett.* **2004**, *92*, 054503-1−054503-4.
(7) Okushima, S.; Nisisako, T.; Torii, T.; Higuchi, T. *Langmuir* **2004**, *20*, 9905−9908.
(8) Nakagawa, K.; Iwamoto, S.; Nakajima, M.; Shono, A.; Satoh, K. *J. Colloid Interface Sci.* **2004**, *278*, 198−205.
(9) Nisisako, T.; Torii, T.; Higuchi, T. *Chem. Eng. J.* **2004**, *101*, 23−29.
(10) Utada, A. S.; Lorenceau, E.; Link, D. R.; Kaplan, P. D.; Weitz, D. A. *Science* **2005**, *308*, 537−541.
(11) Takeuchi, S.; Garstecki, P.; Weibel, D. B.; Whitesides, G. M. *Adv. Mater.* **2005**, *17*, 1067−1072.
(12) Kenis, P. J. A.; Ismagilov, R. F.; Takayama, S.; Whitesides, G. M.; Li, S. L.; White, H. S. *Acc. Chem. Res.* **2000**, *33*, 841−847.
(13) Jeong, W.; Kim, J.; Kim, S.; Lee, S.; Mensing, G.; Beebe, D. J. *Lab Chip* **2004**, *4*, 576−580.
(14) Rolland, J. P.; Van Dam, R. M.; Schorzman, D. A.; Quake, S. R.; DeSimone, J. M. *J. Am. Chem. Soc.* **2004**, *126*, 2322−2323.
(15) Becker, H.; Gartner, C. *Electrophoresis* **2000**, *21*, 12−26.
(16) Poncelet, D.; Alexakis, T.; Desmet, B. P.; Neufeld, R. J. *J. Microencapsulation* **1994**, *11*, 31−40.

JA0529945